



**HAL**  
open science

## Design of fluorescence resonance energy transfer (FRET)-based cGMP indicators: a systematic approach

Michael Russwurm, Florian Mullershausen, Andreas Friebe, Ronald Jäger,  
Corina Russwurm, Doris Koesling

► **To cite this version:**

Michael Russwurm, Florian Mullershausen, Andreas Friebe, Ronald Jäger, Corina Russwurm, et al..  
Design of fluorescence resonance energy transfer (FRET)-based cGMP indicators: a systematic approach. *Biochemical Journal*, 2007, 407 (1), pp.69-77. 10.1042/BJ20070348 . hal-00478771

**HAL Id: hal-00478771**

**<https://hal.science/hal-00478771>**

Submitted on 30 Apr 2010

**HAL** is a multi-disciplinary open access archive for the deposit and dissemination of scientific research documents, whether they are published or not. The documents may come from teaching and research institutions in France or abroad, or from public or private research centers.

L'archive ouverte pluridisciplinaire **HAL**, est destinée au dépôt et à la diffusion de documents scientifiques de niveau recherche, publiés ou non, émanant des établissements d'enseignement et de recherche français ou étrangers, des laboratoires publics ou privés.

## Design of FRET-based cGMP indicators: a systematic approach

**Michael Russwurm, Florian Mullershausen\***, **Andreas Friebe, Ronald Jäger, Corina Russwurm and Doris Koesling<sup>1</sup>**

Institut für Pharmakologie und Toxikologie, Ruhr-Universität Bochum, Universitätsstrasse 150, 44780 Bochum, Germany

\* present address: Novartis Institutes for Biomedical Research, GPCREP, Novartis Pharma AG, Basel, Switzerland.

<sup>1</sup>To whom correspondence should be addressed (e-mail [doris.koesling@ruhr-uni-bochum.de](mailto:doris.koesling@ruhr-uni-bochum.de))

Corresponding Author

Doris Koesling

Institut für Pharmakologie und Toxikologie

Ruhr-Universität Bochum

Universitätsstrasse 150

44780 Bochum, Germany

Tel.: +49 234 32 26827

Fax.: +49 234 32 14521

E-mail: [doris.koesling@ruhr-uni-bochum.de](mailto:doris.koesling@ruhr-uni-bochum.de)

Short title: FRET-based cGMP indicators

## SYNOPSIS

The intracellular signalling molecule cGMP regulates a variety of physiological processes; hence monitoring cGMP dynamics in living cells is highly desirable. Here, we report a systematic approach to create fluorescence resonance energy transfer (FRET)-based cGMP indicators from the two known types of cGMP-binding domains, cNMP-BD and GAF, found in cGMP-dependent protein kinase and phosphodiesterase 5, respectively. Interestingly, only cGMP-binding domains arranged in tandem configuration as in their parent proteins were cGMP-responsive, however, the GAF-derived sensors had to be discarded because of slow kinetics. Out of 24 cGMP-responsive constructs derived from cNMP-BDs, three were selected to cover a range of cGMP affinities with half maximally effective concentrations between 500 nM and 6  $\mu$ M. These indicators feature excellent cGMP specificity, fast kinetics and twice the dynamic range of existing cGMP sensors. The *in vivo* performance of the new indicators is demonstrated in living cells and validated by comparison with cGMP dynamics measured by radioimmunoassays.

Keywords: cGMP biosensor, cGMP-dependent protein kinase, fluorescence resonance energy transfer, phosphodiesterase

## INTRODUCTION

The second messenger cGMP is involved in a variety of physiological processes in mammals, especially in the nervous and vascular systems. Here, cGMP mediates smooth muscle relaxation, inhibition of platelet aggregation and modulation of synaptic plasticity [1-5].

cGMP signals elicited by hormonal stimulation in a given tissue are determined by the cGMP-generating and -degrading enzymes present. Two families of cGMP-generating enzymes exist, the peptide receptor guanylyl cyclases (GC), membrane spanning enzymes activated by peptide hormones like the atrial natriuretic peptide, and the nitric oxide receptor GC activated by the short-lived messenger nitric oxide [6-10]. On the other hand, several families of differentially regulated cGMP-degrading phosphodiesterases are known [11, 12], e.g. PDE1 is stimulated by  $Ca^{++}$  whereas PDE5 is activated by its substrate cGMP. The given combination of GCs and PDEs within specific cell types and even subcellular compartments therefore critically determines amplitude and shape of cGMP signals. The cellular effects of cGMP are conveyed by cGMP-dependent protein kinases [13-15], cGMP-regulated ion channels [16] and by cGMP-regulated phosphodiesterases [1, 12].

With established techniques, the biological effects of cGMP, such as blood vessel relaxation, can be recorded continuously, whereas the cGMP signals themselves can not. Currently, cGMP signals can only be measured subsequent to lysis of cells or tissues by radioimmunoassay (RIA) or enzyme linked immunosorbent-assay (ELISA) using antibodies against cGMP. Hence, a temporal resolution requires determination of tissue cGMP contents at several consecutive time points. Acquiring time courses in this way is laborious, therefore the vast majority of cGMP values reported in the literature were obtained at a single time point, typically as late as 10 minutes after stimulation of the cells or tissues.

On the other hand, accumulating evidence suggests that cGMP signals are of a rather fast and transient nature. Back in 1975, Matsuzawa and Nirenberg [17] reported N1E-115 neuroblastoma cells to respond to carbamylcholine stimulation with a transient up to 200-fold increase in cGMP that lasted for less than 2 minutes. These rapid cGMP kinetics were later confirmed using membrane patches with cyclic nucleotide gated channels crammed into N1E cells [18]. Platelets displayed even faster cGMP signals upon NO stimulation that peaked within 10 s and returned to baseline within 30 s [19, 20]. Thus, indicators that allow continuous monitoring of cGMP concentrations in living cells will substantially improve our knowledge of cyclic nucleotide signalling.

To date, three attempts were made to develop such cGMP indicators. All contained a cGMP-binding domain sandwiched between two fluorescent proteins [21, 22] (Fig. 1) and took advantage of changes in fluorescence resonance energy transfer (FRET) between the fluorophores upon conformational changes caused by cGMP binding. Two different types of cGMP-binding domains are known. One, termed cNMP-BD for cyclic nucleotide

monophosphate binding domain, is conserved in the cGMP-dependent protein kinases (cGK) and the cGMP-regulated ion channels [13, 14]. The second, dubbed GAF domain abbreviating the three proteins in which it was first identified, is in mammals exclusively found in PDEs [23, 24]. Interestingly, two of the cNMP-BD or GAF domains are arranged in tandem in the cGK and PDE, respectively. In cGKI, the N-terminal cNMP-BD, designated cNMP-BD A, has been described as high affinity site whereas cNMP-BD B has a rather low cGMP affinity [25, 26]. In PDE5, the N-terminal GAF domain, GAF-A, binds cGMP leading to activation of the enzyme [27, 28].

The first two cGMP sensors published five years ago used almost the complete cGKI containing both cNMP-BDs lacking only the dimerization domain (47 or 78 amino acids) [29, 30]. Recently, a new attempt was made to generate simpler sensors using a single cNMP-BD from cGKI or a single GAF domain of PDE 2 or 5 [31] (see Fig. 1). The authors reported that only the PDE5 GAF construct responded sufficiently fast for monitoring intracellular cGMP signals.

Taken together, only limited efforts have been made to create cGMP indicators. On one hand, complete cGKs have been used raising the question about the purpose of the catalytic domains in the indicator. On the other hand, only single cGMP-binding domains were tested, albeit both the cGK and PDE each contain these domains in tandem.

Here, we describe a systematic approach to design cGMP indicators using the single and tandem cGMP-binding domains of cGKI (cNMP-BD) and PDE5 (GAF). More than 50 constructs containing different regions of these domains were generated and tested *in vitro*. Based on these data, three indicators containing the tandem cNMP-BD exhibiting cGMP affinities between 500 nM and 6  $\mu$ M were chosen to span a range of cGMP concentrations. The *in vivo* performance of the new indicators is demonstrated by simultaneous measurements of cGMP signals with the new cGMP indicators and radioimmunoassays.

## MATERIALS AND METHODS

**Construction of the sensors.** DNAs encoding the cGMP-binding domains as listed in Tables 1 and 2 were amplified by PCR and subcloned into pcDNA3 containing the coding region of CFP (Clontech's ECFP, equivalent to variant 10C [32], C-terminally truncated at Ala<sup>228</sup>, see below) and YFP (Clontech's EYFP, equivalent to variant W1B [32]), using the type IIa restriction endonuclease Esp3I. In the resulting protein sequence, the cGMP-binding domain (see. Tabs. 1 and 2) is directly preceded by the C-terminal end of CFP (...Thr<sup>226</sup>Ala<sup>227</sup>Ala<sup>228</sup>-) and followed by YFP (-Met<sup>1</sup>Val<sup>2</sup>Ser<sup>3</sup>...) without any additional amino acids, respectively. To allow screening of a larger number of constructs, only some of them were verified by sequencing (showing no mutations at all).

***In vitro* characterization.** The indicators were transiently expressed in HEK-293 cells using Fugene6 according to the manufacturer's instructions (Roche). Transfected cells ( $1 \times 10^7$ ) were harvested and lysed in homogenization buffer (50 mM NaCl, 1 mM EDTA, 50 mM triethanolamine/HCl, pH 7.4, containing 2 mM dithiothreitol and a 100-fold dilution of protease inhibitor cocktail, Sigma-Aldrich) by sonication (1 pulse, 5 s). A cytosolic fraction was obtained ( $100,000 \times g$ , 30 min, 4 °C) and emission spectra were recorded using a Cary eclipse spectrofluorometer (Varian Inc., excitation at 436 nm). In brief, 10 to 100  $\mu$ l of the cytosol containing the indicators were measured in a total volume of 800  $\mu$ l buffer A (25 or 50 mM triethanolamine/HCl, pH 7.4, 2 mM dithiothreitol, 10 mM MgCl<sub>2</sub>). Concentration response curves for cGMP and cAMP were assessed by continuous recording of CFP and YFP emissions at 475 and 525 nm, respectively, and calculating the emission ratio at 475 to 525 nm (data presented are means  $\pm$  S.D. of  $\geq 3$  measurements). Binding kinetics were recorded at an emission of 525 nm using an Applied Photophysics RX.2000 stopped flow device connected to the spectrofluorometer. For the dissociation measurements, binding of cGMP at the indicated concentrations was confirmed by emission ratio change. Subsequently, 8  $\mu$ l of the cGMP-bound indicator were diluted with buffer A to 800  $\mu$ l to lower the cGMP concentration, and emission changes (475 and 525 nm) were recorded.

***In vivo* measurements.** HEK-293 cells stably expressing the NO receptor GC and PDE5 were cultured as described [33]. Measurements were performed at room temperature after replacing the cell culture medium by PBS. Cells were stimulated with DEA-NO (200  $\mu$ M) and YC-1 (20  $\mu$ M) at the time points indicated and subsequently cGMP contents were determined by RIA as described [33]. For fluorescence microscopy, the cells were grown on coverslips and transfected with the indicators as described above. After mounting the coverslips onto the microscope stage, cells were maintained at room temperature in PBS and stimulated as described above. Calibration was attempted by the use of 10  $\mu$ M of the cGMP analogues 8-(4-Chlorophenylthio)guanosine-3',5'-cyclic monophosphate (8-pCPT-cGMP),  $\beta$ -Phenyl-1,N<sup>2</sup>-etheno-8-bromoguanosine-3',5'-cyclic monophosphate (8-Br-PET-cGMP), 8-(4-Chloro-

phenylthio)- $\beta$ -phenyl-1, $N^2$ -ethenoguanosine-3',5'-cyclicmonophosphorothioate, Sp-isomer (Sp-8-pCPT-PET-cGMPS). Dual emission fluorescence microscopy was performed on a Zeiss Axiovert 200 equipped with a Fucal 4 system (Till Photonics) and a Dual View beam splitter (Optical insights) for simultaneous recording of CFP and YFP emissions. Recordings were done with excitation set to 436 nm, integration time 2 s, 10 $\times$  objective. Data were analyzed using NIH ImageJ. Each field of view contained approximately 20 cells; to circumvent an observer bias due to manual selection of regions of interest, all pixels exhibiting in the first captured frame >20% of the fluorescence of average bright cells were used for analysis. For each pixel, the CFP/YFP emission ratio was calculated. Mean CFP and YFP intensities and mean CFP/YFP emission ratio of the viewing field were calculated from all pixels selected as described above and normalized to the initial baseline values, respectively. Estimations of the intracellular cGMP concentrations were performed by fitting the *in vitro* concentrations response curves with a four parameter logistic function. Subsequently, the obtained  $EC_{50}$  and Hill constant were applied together with the maximum and minimum FRET values obtained *in vivo* to the inverse four-parameter logistic function to yield the intracellular cGMP concentrations.

## RESULTS

To generate genetically encoded indicators for cGMP measurements in living cells, different cGMP-binding domains were sandwiched between two fluorescent proteins, CFP and YFP.

### **PDE5-derived constructs are too slow for detection of cGMP signals**

First, we tried to design cGMP indicators from PDE5 using the single GAF A as well as the tandem of GAF A + B (see Fig. 1). Our attempt to select regions according to the crystal structure of the PDE2 GAF domains [34] was unsuccessful, i.e. the constructs did not show cGMP-induced FRET changes. This may be due to the small number of conserved amino acids between the GAF domains of PDE2 and PDE5 resulting in relatively vague GAF borders. Thus, in a trial-and-error approach we elongated or shortened either the GAF A or the combined GAF A + B domains repetitively by approx. 10 amino acids on their N and C termini (Tab. 1). These constructs were expressed in HEK293 cells and characterized *in vitro*, i.e. the change in the CFP/YFP emission ratio upon addition of cGMP was recorded in cytosolic fractions (see Tab. 1). Interestingly, as much as 51 amino acids had to be added N-terminally of the combined GAF A + B domain of PDE5 to create a functional, cGMP-responsive construct. This construct responded with an 80% increase in CFP/YFP emission ratio to addition of 100  $\mu$ M cGMP. Further elongation at either end decreased the cGMP-induced fractional change. Any deletion at the C-terminus abolished cGMP-induced FRET changes. None of the constructs containing a single GAF A responded to cGMP with a FRET change.

Therefore, PDE5-GAF A + B, N-terminally elongated by 51 amino acids and C-terminally shortened by 2 amino acids, (see Tab. 1) was further characterized. First, concentration response curves of the construct were obtained yielding an apparent  $EC_{50}$  of 0.3  $\mu$ M cGMP (Fig. 2A). The construct was selective for cGMP; up to 100  $\mu$ M of cAMP did not elicit a FRET change (see Fig. 2A). However, while recording the cGMP concentration response curves, we realized that the construct responded rather slowly to low concentrations of cGMP. Thus, kinetics of cGMP binding were assessed (Fig. 2B). Although binding at 10  $\mu$ M cGMP occurred with a half life of 0.7 s, 10- and 100-fold lower concentrations yielded half lives of 14 s and 120 s, as also predicted by the law of mass action. Slow binding at low cGMP concentrations does not render the constructs inadequate for *in vivo* measurements *per se*; however, fast dissociation of cGMP is essential. To assess dissociation kinetics, the construct was incubated with 1  $\mu$ M cGMP, subsequently the free cGMP concentration was reduced by a 100-fold dilution and FRET changes were recorded (Fig. 2C). Under these conditions, complete reversal of the signal required 1 hour with a calculated half life of approx. 10 min. A similar dissociation half life can be calculated from the binding experiments. In sum, we were not able to create a functional cGMP sensor from the single PDE5 GAF A; the combined

GAF A + B domains of PDE5 yielded a sensor with pronounced cGMP-induced FRET changes but intolerably slow binding and dissociation kinetics.

### **cGMP indicators derived from cGK display fast kinetics**

Next, we reevaluated the already existing cGMP sensors containing almost the complete cGKI [30] and found much faster binding kinetics than with the GAF constructs *in vitro* (not shown). Therefore, we decided to construct cGMP indicators from the cNMP-BD of cGKI. The margins of the cNMP-BD were deduced from the cAMP-binding domains of the cAMP-dependent protein kinase crystallized 10 years ago [35]. To circumvent extremely low cGMP affinities, we used cGKI's high affinity cNMP-BD A [25, 26] and the tandem of cNMP-BD A + B for construction of the indicators (see Fig. 1). As described for the GAF domains of PDE5, we screened for cGMP-induced FRET changes and characterized functional, cGMP-responsive constructs with regards to cGMP affinity (Tab. 2). As with the GAF domains, the single cNMP-BD A did not produce functional indicators. However, constructs composed of both cNMP-BD A + B responded to cGMP with an up to 80% increase in CFP/YFP emission ratio. Based on cGMP affinity and extent of FRET change, three **cGMP** indicators were selected covering a range of half maximally effective cGMP concentrations of 500 nM, 3  $\mu$ M and 6  $\mu$ M and termed cGi-500, cGi-3000 and cGi-6000, respectively (Fig. 3A). cGi-500 and cGi-3000 responded with pronounced FRET changes (77% and 72% increase, respectively), whereas cGi-6000 had a somewhat lower dynamic range of 57%. The constructs were highly selective for cGMP, up to 1 mM cAMP elicited only marginal emission increases (Fig. 3B). Next, we assessed the binding and dissociation kinetics. Using stopped flow instrumentation with a dead time of 80 ms, we were not able to monitor binding kinetics, i.e. binding was complete within the dead time of the instrument (not shown). As with the GAF constructs, dissociation was characterized by a 100-fold dilution of the cGMP-bound indicators. In contrast to the GAF construct (see Fig. 2C), dissociation was complete within the mixing time (Fig. 3C) clearly showing that these cGMP indicators are fast enough to monitor intracellular cGMP signals.

### **The new cGMP indicators detect cGMP signals *in vivo***

HEK293 cells stably expressing NO-sensitive GC and PDE5 [33] were used to demonstrate the *in vivo* performance of the cGMP indicators. These cells show transient up to 300-fold cGMP increases upon NO application that are reversible within 5 min as demonstrated by cGMP measurements in radioimmunoassays (Fig. 4A). The cGMP signals in these cells are reminiscent of those in platelets and smooth muscle cells, which also show several ten fold increases in cGMP that rapidly return to almost basal levels within seconds to minutes [19]. Since sustained activation of PDE5 outlasts the cGMP signals by far, the cells can not be restimulated with NO. However, YC-1, a combined GC activator and PDE inhibitor [36, 37], overcomes the activation of PDE5 and again increases cGMP levels (see Fig. 4A).

These cells were transfected with the cGMP indicators and FRET changes were recorded by fluorescence microscopy of living cells. The three indicators mirrored the transient cGMP elevations elicited by NO and YC-1: The NO-induced cGMP elevation immediately produced a sharp increase in the CFP/YFP emission ratio which reached a plateau after 30-40 s and remained constant during the next 3 min suggesting full saturation of the indicators (Figs. 4B-D and Supplementary Video 1). Thereafter, the cGMP levels declined (see Fig. 4A) and the indicators followed that decline according to their cGMP affinities, i.e. the most sensitive indicator, cGi-500, displayed a minor decrease in emission ratio, whereas the indicator with the lowest affinity, cGi-6000 decreased to almost basal level (see Figs. 4B and D). The subsequent cGMP elevation elicited by YC-1 (see Fig. 4A) is reflected by the three indicators and again saturated cGi-500 and -3000.

In order to calibrate the obtained FRET signals to cGMP concentrations, we considered the application of membrane permeable cGMP analogues. We first ensured that the cGMP analogues bind to the cGMP indicators and generate FRET changes comparable to cGMP by *in vitro* analysis (not shown). Then, we applied the cGK activators to the HEK cell line and recorded the CFP/YFP emission ratio as described above for 5 min, followed by NO administration as control. Unfortunately, none of the membrane permeable cGMP analogues tested (8-pCPT-cGMP, 8-Br-PET-cGMP, Sp-8-pCPT-cGMPS) elicited any FRET response, whereas the control NO application produced the same signals as described above.

Although calibration was therefore impossible, an estimation of the intracellular cGMP concentration is nevertheless feasible as the extent of FRET change and the oblate peaks observed with the three indicators are indicative of cGMP-free indicators before application of NO and full saturation at the peak cGMP concentrations after NO stimulation, respectively. On the basis of the cGMP concentration response curves determined *in vitro* (see Fig. 3A), the intracellular cGMP concentrations underlying the FRET responses were calculated and depicted as second ordinate (see Figs. 4B-D). The resting and peak intracellular cGMP concentrations can not be deduced from these axes because they fall into the horizontal parts of the sigmoid standard curve. However, the cGMP concentration of the plateau after the peak elicited by NO (300-400s) can be read to be 1 to 2  $\mu\text{M}$  as measured with the three indicators (compare Figs. 4B-D).

In sum, the congruence of the cGMP signals determined by RIA and fluorescence microscopy clearly demonstrates the *in vivo* applicability of the indicators. Quantification of intracellular cGMP concentrations is only possible if the cGMP concentration can be brought to a level that leads to saturation of the indicators.

## DISCUSSION

Conventional analysis of cGMP signalling requires disruption of the cells or tissues and subsequent detection of cGMP e.g. by RIA. Although a moderate temporal resolution can be achieved, spatial resolution is lost by integration of the signal over many cells. These limitations initiated the development of fluorescent indicators for real time measurement of cGMP in living cells.

For this purpose, cGMP-binding domains were sandwiched between two fluorescent proteins (see Fig. 1). Two substantially different cGMP-binding domains are known. The first one, cNMP-BD, is conserved in the cGK and the cGMP-regulated ion channels. The second one, GAF, is in mammals found in PDEs.

Because earlier indicators derived from the cGKI apparently had a low temporal resolution [30], we first tried to use GAF domains for development of cGMP indicators. The GAF domains of PDE5 were selected because among the PDE GAF domains they show the highest specificity for cGMP vs. cAMP. We generated a series of constructs from the single GAF A domain; however, none of these constructs showed cGMP-induced FRET changes. Furthermore, a range of constructs containing the tandem of GAF A + B was characterized. Interestingly, solely constructs containing not only the two GAF domains but also the PDE5 phosphorylation site located 42 amino acids N-terminally of the GAF domains showed cGMP-induced conformational changes. The requirement for the phosphorylation site is not obvious; together with biochemical data from the holoenzyme these findings suggest that the phosphorylation site is in close proximity to the GAF domains and released upon cGMP binding [28]. Disappointingly, the conformational changes of these GAF-derived constructs were rather slow. At 100 nM cGMP, completion of the FRET change took more than a minute. More than an hour was required for cGMP dissociation. Such slow kinetics renders the constructs inappropriate for monitoring intracellular cGMP signals that are much faster.

Therefore, we decided to create constructs from the other type of cGMP-binding domains, the cNMP-BD of cGKI. Similar to the tandem GAF domains in the PDE, cGKI contains two cNMP-BDs in the N-terminal regulatory region. Besides these two cNMP-BDs, the already published cGKI indicators also contained the C-terminal kinase catalytic region as only either N- or C-terminal deletions were performed and the tested C-terminal truncations were reported to cause irreversible FRET changes upon cGMP binding [30]. However, by simultaneous N- and C-terminal truncations, we obtained indicators containing the cNMP-BD only. As with the GAF domains, a tandem of two cGMP-BDs was required to produce a functional indicator (see Tab. 2). Further elongation and shortening produced a range of functional indicators differing in dynamic range and cGMP affinity. To cover a spectrum of cGMP affinities, three **cGMP** indicators were selected and named according to their  $EC_{50}$ , cGi-500, -3000 and -6000. The indicators exhibit fast binding and dissociation kinetics, an

excellent selectivity for cGMP vs. cAMP and a twofold greater dynamic range than earlier described cGMP sensors (Tab. 3).

Both cNMP-BD were required to obtain cGMP-responsive constructs. In the cGK holoenzyme, both sites have been shown to bind cGMP. While the sites have different affinities and exhibit cooperativity in cGKI $\alpha$ , the matter is controversial for cGKI $\beta$  [38, 39]. The N-terminal parts preceding the cNMP-BD are the only regions differing between cGKI $\alpha$  and  $\beta$  and have been shown to be responsible for the different cGMP binding properties [39, 40]. Furthermore, proteolytic removal of cGKI $\alpha$  amino acids preceding Gln<sup>79</sup> has been described to eliminate cooperativity [41]. As the cGMP indicators do not contain this N-terminal region, non-cooperative binding would be predicted. Indeed, the concentration response curves of the indicators displayed hill coefficients of  $\leq 1$  arguing against cooperativity. On the basis of available data from the cGK holoenzyme, the indicators can be assumed to bind two molecules cGMP each. Whether the two sites have similar affinities or whether the conformational change is brought about by occupation of the low affinity site can not be decided on the basis of our data.

The *in vivo* applicability of the indicators is demonstrated by fluorescence microscopy measurements in a well characterized cellular system. As most of the cultured cell lines contain no or very little NO-sensitive GC, we used a HEK293 cell line that stably expresses the NO receptor GC and PDE5 and shows transient cGMP signals comparable to those in platelets and smooth muscle cells. As shown in radioimmunoassays, the cell line responds to NO stimulation with a steep, more than 100-fold increase in cGMP that is reversed within 5 min. The three indicators detected the cGMP increase immediately and reached a plateau at the highest cGMP levels. The following decline in cGMP was reflected differently by the indicators according to their cGMP sensitivity.

Since the indicators reached a plateau, they may be suspected to be too sensitive. However, maximally activating NO concentrations had to be used in order to elicit cGMP increases that are reliably detectable by RIA. In contrast, physiological effects of NO are regularly observed without cGMP elevations detectable by RIA [42, 43]. Determination of those minute cGMP elevations demands the development of very sensitive indicators. Because the affinity of cGi-500 equals the one of the most important cGMP effector molecule, cGK, it permits detection of cGMP elevations relevant to activation of cGMP effector molecules. The indicators described here feature a hill slope of 1 and therefore can detect cGMP increases of 1 to 1.5 orders of magnitude with sufficient resolution. If the indicators are able to monitor physiologically relevant cGMP levels leading to activation of cGK, they inevitably cannot resolve the peak cGMP concentrations elicited by maximally activating NO concentrations required to produce cGMP signals detectable by RIA.

Standardisation of FRET-signals obtained with bio-indicators to the underlying biological signals is usually obtained by internal calibration [22]. To do so, the intracellular

concentration of the biomolecule to be measured has to be clamped to low and high concentrations; together with the  $EC_{50}$  of the indicator obtained in *in vitro* experiments, the intracellular concentration of the biomolecule can be calculated. For  $Ca^{2+}$  indicators this type of calibration is performed by using chelators and ionophores, however similar tools for the manipulation of cyclic nucleotide levels inside cells are not available. Therefore, the use of activators and inhibitors of cGK, i.e. agonists and antagonists of the cNMP-BD, appeared to be the only way to force the cGMP indicators to the cGMP-bound and -free states. We tested several membrane permeable analogues but apparently the intracellular concentrations reached were not sufficient to elicit FRET responses. Physiological responses to these membrane permeable activators are well established. Therefore, this result was unexpected but can be explained by the fact that physiological responses already occur at low intracellular concentrations leading to activation of only some cGK molecules, whereas a substantial portion of the FRET indicators molecules has to become bound to produce a detectable FRET signal.

FRET-based indicators for intracellular cGMP have been constructed before. The 'cygnet' [30] and 'cgy' [29] sensors described 5 years ago contained almost the complete cGK which positioned the fluorophores in larger distance resulting in smaller FRET changes compared to the indicators described here (see Fig. 1 and Tab. 3). It remains unclear why deletion of the kinase catalytic domain was described to cause irreversible FRET changes upon cGMP binding [30] as this was not the case in our hands. Recently, a sensor, termed cGES-DE5, made up of the GAF A domain of PDE5 was published to have superior properties compared to the cygnet sensors [31]. Although our GAF A constructs differ by less than 10 amino acids from the cGES-DE5, they showed negligible cGMP-induced FRET changes. Furthermore, our functional constructs containing the tandem GAF A + B domains of PDE5 had rather slow kinetics. The reasons for these discrepancies are unknown and may be attributed to the differences between the constructs. However, the fluorescence emission spectra of cGES-DE5 published (Supplement to [31]) indicate an only 20% change in the uncorrected emission ratio in response to cGMP (see Tab. 3).

Taken together, in a systematic approach the two known types of cGMP-binding domains were tested for their suitability to serve as cGMP indicators by fusing different fragments of the domains to two fluorescent proteins. Constructs containing GAF domains of PDE5 exhibited extremely slow binding and dissociation kinetics. Three cGMP indicators based on the tandem of cNMP-BD A + B of cGK were generated that respond fast and reversibly to cGMP, display a high specificity for cGMP over cAMP and cover a range of cGMP affinities between 500 nM and 6  $\mu$ M. With the help of these indicators, physiologically relevant cGMP signals that remain undetected with current techniques will be unveiled as will be cGMP signals in subcellularly confined signalling microdomains.

## **ACKNOWLEDGMENTS**

We thank Ulla Krabbe, Erika Mannheim and Arkadius Pacha for technical assistance, and Michael Schaefer for technical advice. This work was supported by grants of the Deutsche Forschungsgemeinschaft (Ko1157) and the Kommission für Finanzautonomie und Ergänzungsmittel of the medical faculty (KOFFER).

## **ABBREVIATIONS**

cGK, cGMP-dependent protein kinase; cNMP-BD, cyclic nucleotide monophosphate binding domain of cGK; FRET, fluorescence resonance energy transfer; GC, guanylyl cyclase; PDE, phosphodiesterase, RIA, radioimmunoassay

## REFERENCES

- 1 Rybalkin, S. D., Yan, C., Bornfeldt, K. E. and Beavo, J. A. (2003) Cyclic GMP phosphodiesterases and regulation of smooth muscle function. *Circ. Res.* **93**, 280-91
- 2 Feil, R., Lohmann, S. M., de Jonge, H., Walter, U. and Hofmann, F. (2003) Cyclic GMP-dependent protein kinases and the cardiovascular system: insights from genetically modified mice. *Circ. Res.* **93**, 907-16
- 3 Münzel, T., Feil, R., Mulsch, A., Lohmann, S. M., Hofmann, F. and Walter, U. (2003) Physiology and pathophysiology of vascular signaling controlled by guanosine 3',5'-cyclic monophosphate-dependent protein kinase. *Circulation* **108**, 2172-83
- 4 Garthwaite, J. and Boulton, C. L. (1995) Nitric oxide signaling in the central nervous system. *Annu. Rev. Physiol.* **57**, 683-706
- 5 Lev-Ram, V., Jiang, T., Wood, J., Lawrence, D. S. and Tsien, R. Y. (1997) Synergies and coincidence requirements between NO, cGMP, and Ca<sup>2+</sup> in the induction of cerebellar long-term depression. *Neuron* **18**, 1025-38
- 6 Kuhn, M. (2005) Cardiac and intestinal natriuretic peptides: insights from genetically modified mice. *Peptides* **26**, 1078-85
- 7 Lucas, K. A., Pitari, G. M., Kazerounian, S., Ruiz-Stewart, I., Park, J., Schulz, S., Chepenik, K. P. and Waldman, S. A. (2000) Guanylyl cyclases and signaling by cyclic GMP. *Pharmacol. Rev.* **52**, 375-414
- 8 Wedel, B. and Garbers, D. (2001) The guanylyl cyclase family at Y2K. *Annu. Rev. Physiol.* **63**, 215-33
- 9 Friebe, A. and Koesling, D. (2003) Regulation of nitric oxide-sensitive guanylyl cyclase. *Circ. Res.* **93**, 96-105
- 10 Hobbs, A. J. (2002) Soluble guanylate cyclase: an old therapeutic target re-visited. *Br. J. Pharmacol.* **136**, 637-40
- 11 Bender, A. T. and Beavo, J. A. (2006) Cyclic nucleotide phosphodiesterases: molecular regulation to clinical use. *Pharmacol. Rev.* **58**, 488-520
- 12 Francis, S. H., Turko, I. V. and Corbin, J. D. (2001) Cyclic nucleotide phosphodiesterases: relating structure and function. *Prog. Nucleic. Acid Res. Mol. Biol.* **65**, 1-52
- 13 Pfeifer, A., Ruth, P., Dostmann, W., Sausbier, M., Klatt, P. and Hofmann, F. (1999) Structure and function of cGMP-dependent protein kinases. *Rev. Physiol. Biochem. Pharmacol.* **135**, 105-49
- 14 Francis, S. H. and Corbin, J. D. (1999) Cyclic nucleotide-dependent protein kinases: intracellular receptors for cAMP and cGMP action. *Crit. Rev. Clin. Lab. Sci.* **36**, 275-328
- 15 Eigenthaler, M., Lohmann, S. M., Walter, U. and Pilz, R. B. (1999) Signal transduction by cGMP-dependent protein kinases and their emerging roles in the regulation of cell adhesion and gene expression. *Rev. Physiol. Biochem. Pharmacol.* **135**, 173-209

- 16 Biel, M., Zong, X., Ludwig, A., Sautter, A. and Hofmann, F. (1999) Structure and function of cyclic nucleotide-gated channels. *Rev. Physiol. Biochem. Pharmacol.* **135**, 151-71
- 17 Matsuzawa, H. and Nirenberg, M. (1975) Receptor-mediated shifts in cGMP and cAMP levels in neuroblastoma cells. *Proc. Nat. Acad. Sci. U S A* **72**, 3472-6
- 18 Trivedi, B. and Kramer, R. H. (1998) Real-time patch-clamp detection of intracellular cGMP reveals long-term suppression of responses to NO and muscarinic agonists. *Neuron* **21**, 895-906
- 19 Mullershausen, F., Russwurm, M., Thompson, W. J., Liu, L., Koesling, D. and Friebe, A. (2001) Rapid nitric oxide-induced desensitization of the cGMP response is caused by increased activity of phosphodiesterase type 5 paralleled by phosphorylation of the enzyme. *J. Cell. Biol.* **155**, 271-8
- 20 Mo, E., Amin, H., Bianco, I. H. and Garthwaite, J. (2004) Kinetics of a cellular nitric oxide/cGMP/phosphodiesterase-5 pathway. *J. Biol. Chem.* **279**, 26149-58
- 21 Zhang, J., Campbell, R. E., Ting, A. Y. and Tsien, R. Y. (2002) Creating new fluorescent probes for cell biology. *Nat. Rev. Mol. Cell. Biol.* **3**, 906-18
- 22 Miyawaki, A. and Tsien, R. Y. (2000) Monitoring protein conformations and interactions by fluorescence resonance energy transfer between mutants of green fluorescent protein. *Methods Enzymol.* **327**, 472-500
- 23 Aravind, L. and Ponting, C. P. (1997) The GAF domain: an evolutionary link between diverse phototransducing proteins. *Trends Biochem. Sci.* **22**, 458-9
- 24 Martinez, S. E., Beavo, J. A. and Hol, W. G. (2002) GAF Domains: Two-Billion-Year-Old Molecular Switches that Bind Cyclic Nucleotides. *Mol. Interv.* **2**, 317-23
- 25 Reed, R. B., Sandberg, M., Jahnsen, T., Lohmann, S. M., Francis, S. H. and Corbin, J. D. (1996) Fast and slow cyclic nucleotide-dissociation sites in cAMP-dependent protein kinase are transposed in type I $\beta$  cGMP-dependent protein kinase. *J. Biol. Chem.* **271**, 17570-5
- 26 Reed, R. B., Sandberg, M., Jahnsen, T., Lohmann, S. M., Francis, S. H. and Corbin, J. D. (1997) Structural order of the slow and fast intrasubunit cGMP-binding sites of type I  $\alpha$  cGMP-dependent protein kinase. *Adv. Second Messenger Phosphoprotein Res.* **31**, 205-17
- 27 Rybalkin, S. D., Rybalkina, I. G., Shimizu-Albergine, M., Tang, X. B. and Beavo, J. A. (2003) PDE5 is converted to an activated state upon cGMP binding to the GAF A domain. *EMBO J.* **22**, 469-78
- 28 Zoraghi, R., Bessay, E. P., Corbin, J. D. and Francis, S. H. (2005) Structural and functional features in human PDE5A1 regulatory domain that provide for allosteric cGMP binding, dimerization, and regulation. *J. Biol. Chem.* **280**, 12051-63
- 29 Sato, M., Hida, N., Ozawa, T. and Umezawa, Y. (2000) Fluorescent indicators for cyclic GMP based on cyclic GMP-dependent protein kinase I $\alpha$  and green fluorescent proteins. *Anal. Chem.* **72**, 5918-24

- 30 Honda, A., Adams, S. R., Sawyer, C. L., Lev-Ram, V., Tsien, R. Y. and Dostmann, W. R. (2001) Spatiotemporal dynamics of guanosine 3',5'-cyclic monophosphate revealed by a genetically encoded, fluorescent indicator. *Proc. Nat. Acad. Sci. U S A* **98**, 2437-42
- 31 Nikolaev, V. O., Gambaryan, S. and Lohse, M. J. (2006) Fluorescent sensors for rapid monitoring of intracellular cGMP. *Nat. Methods* **3**, 23-5
- 32 Tsien, R. Y. (1998) The green fluorescent protein. *Annu. Rev. Biochem.* **67**, 509-44
- 33 Mullershausen, F., Russwurm, M., Koesling, D. and Friebe, A. (2004) In vivo reconstitution of the negative feedback in nitric oxide/cGMP signaling: role of phosphodiesterase type 5 phosphorylation. *Mol. Biol. Cell* **15**, 4023-30
- 34 Martinez, S. E., Wu, A. Y., Glavas, N. A., Tang, X. B., Turley, S., Hol, W. G. and Beavo, J. A. (2002) The two GAF domains in phosphodiesterase 2A have distinct roles in dimerization and in cGMP binding. *Proc. Nat. Acad. Sci. U S A* **99**, 13260-5
- 35 Su, Y., Dostmann, W. R., Herberg, F. W., Durick, K., Xuong, N. H., Ten Eyck, L., Taylor, S. S. and Varughese, K. I. (1995) Regulatory subunit of protein kinase A: structure of deletion mutant with cAMP binding domains. *Science* **269**, 807-13
- 36 Friebe, A., Mullershausen, F., Smolenski, A., Walter, U., Schultz, G. and Koesling, D. (1998) YC-1 potentiates nitric oxide- and carbon monoxide-induced cyclic GMP effects in human platelets. *Mol. Pharmacol.* **54**, 962-7
- 37 Galle, J., Zabel, U., Hubner, U., Hatzelmann, A., Wagner, B., Wanner, C. and Schmidt, H. H. (1999) Effects of the soluble guanylyl cyclase activator, YC-1, on vascular tone, cyclic GMP levels and phosphodiesterase activity. *Br. J. Pharmacol.* **127**, 195-203
- 38 Wolfe, L., Corbin, J. D. and Francis, S. H. (1989) Characterization of a novel isozyme of cGMP-dependent protein kinase from bovine aorta. *J. Biol. Chem.* **264**, 7734-41
- 39 Ruth, P., Landgraf, W., Keilbach, A., May, B., Egleme, C. and Hofmann, F. (1991) The activation of expressed cGMP-dependent protein kinase isozymes I  $\alpha$  and I  $\beta$  is determined by the different amino-termini. *Eur. J. Biochem.* **202**, 1339-44
- 40 Ruth, P., Pfeifer, A., Kamm, S., Klatt, P., Dostmann, W. R. and Hofmann, F. (1997) Identification of the amino acid sequences responsible for high affinity activation of cGMP kinase I $\alpha$ . *J. Biol. Chem.* **272**, 10522-8
- 41 Heil, W. G., Landgraf, W. and Hofmann, F. (1987) A catalytically active fragment of cGMP-dependent protein kinase. Occupation of its cGMP-binding sites does not affect its phosphotransferase activity. *Eur. J. Biochem.* **168**, 117-21
- 42 Mullershausen, F., Lange, A., Mergia, E., Friebe, A. and Koesling, D. (2006) Desensitization of NO/cGMP signaling in smooth muscle: blood vessels versus airways. *Mol. Pharmacol.* **69**, 1969-74
- 43 Mergia, E., Friebe, A., Dangel, O., Russwurm, M. and Koesling, D. (2006) Spare guanylyl cyclase NO receptors ensure high NO sensitivity in the vascular system. *J. Clin. Invest.* **116**, 1731-7
- 44 Wernet, W., Flockerzi, V. and Hofmann, F. (1989) The cDNA of the two isoforms of bovine cGMP-dependent protein kinase. *FEBS Lett.* **251**, 191-6

**TABLES**
**Table 1 FRET constructs derived from the GAF domains of PDE5**

Shown are the relative changes in CFP/YFP emission ratio of the constructs derived from the PDE5 GAF domains determined *in vitro* as described under *Materials and Methods*. The borders of the constructs containing either GAF A + B or GAF A (see Fig. 1) are given relative to the border of the GAF domains (given in the left column) of human PDE5a (NM\_001083.2). The first and the last amino acid (aa) relative to the PDE5 holoenzyme are given in parentheses. n.d., not determined because the constructs displayed a very low expression.

	<b>N-terminal elongation (1<sup>st</sup> aa)</b>	<b>C-terminal elongation (last aa)</b>	<b>change in CFP/YFP emission ratio</b>
<b>GAF A + B</b> (Asp <sup>144</sup> – Ala <sup>517</sup> )	+60 (Gln <sup>84</sup> )	+10 (Ser <sup>527</sup> )	<b>50%</b>
	+51 (Val <sup>93</sup> )	-23 (Ala <sup>494</sup> )	< 5%
		-10 (Gln <sup>507</sup> )	< 5%
		-2 (Ala <sup>515</sup> )	<b>80%</b>
		+10 (Ser <sup>527</sup> )	<b>40%</b>
		+27 (Ala <sup>544</sup> )	<b>30%</b>
	+44 (Lys <sup>100</sup> )	-23 (Ala <sup>494</sup> )	< 5%
		-16 (Leu <sup>501</sup> )	< 5%
		-10 (Gln <sup>507</sup> )	< 5%
		-2 (Ala <sup>515</sup> )	< 5%
		+10 (Ser <sup>527</sup> )	< 5%
		+12 (His <sup>529</sup> )	< 5%
	+30 (Val <sup>114</sup> )	-2 (Ala <sup>515</sup> )	< 5%
+10 (Ser <sup>527</sup> )		< 5%	
+21 (Ser <sup>123</sup> )	-2 (Ala <sup>515</sup> )	< 5%	
	+10 (Ser <sup>527</sup> )	< 5%	
+10 (Met <sup>134</sup> )	-31 (Arg <sup>486</sup> )	< 5%	
	-2 (Ala <sup>515</sup> )	< 5%	
	+10 (Ser <sup>527</sup> )	< 5%	
0 (Asp <sup>144</sup> )	-16 (Leu <sup>501</sup> )	7%	
	+12 (His <sup>529</sup> )	< 5%	
-10 (Glu <sup>154</sup> )	-31 (Arg <sup>486</sup> )	n. d.	
<b>GAF A</b> (Asp <sup>144</sup> – Ile <sup>312</sup> )	+60 (Gln <sup>84</sup> )	+14 (Glu <sup>326</sup> )	< 5%
	+51 (Val <sup>93</sup> )	-19 (Gly <sup>293</sup> )	< 5%
		+2 (Leu <sup>314</sup> )	< 5%
		+14 (Glu <sup>326</sup> )	< 5%
		+35 (Leu <sup>347</sup> )	< 5%
	+21 (Ser <sup>123</sup> )	+2 (Leu <sup>314</sup> )	< 5%
		+14 (Glu <sup>326</sup> )	< 5%
	0 (Asp <sup>144</sup> )	+2 (Leu <sup>314</sup> )	< 5%
		+14 (Glu <sup>326</sup> )	< 5%
		+26 (Ser <sup>338</sup> )	< 5%
		+35 (Leu <sup>347</sup> )	< 5%
	-21 (Val <sup>165</sup> )	+2 (Leu <sup>314</sup> )	n. d.
+14 (Glu <sup>326</sup> )		< 5%	

**Table 2 FRET constructs derived from the cNMP-BD of cGKI**

Shown are the relative changes in CFP/YFP emission ratio of the constructs derived from the cNMP-BD of cGKI determined *in vitro* as described under *Materials and Methods*. The borders of the constructs containing either cNMP-BD A + B or cNMP-BD A (see Fig. 1) are given relative to the border of the cNMP-BD (given in the left column) of bovine cGKI (X16086.1 [44]). The first and the last amino acid (aa) relative to the cGKI holoenzyme are given in parentheses. Values are means  $\pm$  SEM of  $\geq 3$  independent experiments. EC<sub>50</sub>, half-maximally effective concentration; n.d., not determined because no ratio change was detectable.

	N-terminal elongation (1 <sup>st</sup> aa)	C-terminal elongation (last aa)	change in CFP/YFP emission ratio	EC <sub>50</sub> ( $\mu$ M)		
cNMP-BD A + B (Gln <sup>79</sup> – Tyr <sup>336</sup> )	+45 (Gln <sup>34</sup> )	0 (Tyr <sup>336</sup> ) +9 (Tyr <sup>345</sup> )	29 $\pm$ 3% 27 $\pm$ 2%	1.47 $\pm$ 0.44 0.64 $\pm$ 0.19		
	+35 (Gln <sup>44</sup> )	0 (Tyr <sup>336</sup> ) +9 (Tyr <sup>345</sup> )	42 $\pm$ 2% 45 $\pm$ 2%	1.25 $\pm$ 0.20 0.23 $\pm$ 0.04		
	+23 (Pro <sup>56</sup> )	0 (Tyr <sup>336</sup> ) +9 (Tyr <sup>345</sup> )	56 $\pm$ 2% 55 $\pm$ 3%	1.11 $\pm$ 0.13 0.27 $\pm$ 0.02		
	+12 (Glu <sup>67</sup> )	0 (Tyr <sup>336</sup> ) +9 (Tyr <sup>345</sup> )	66 $\pm$ 2% 55 $\pm$ 3%	1.57 $\pm$ 0.04 0.50 $\pm$ 0.06		
	+5 (Phe <sup>74</sup> )	0 (Tyr <sup>336</sup> ) +9 (Tyr <sup>345</sup> )	62 $\pm$ 3% 69 $\pm$ 2%	1.32 $\pm$ 0.07 0.33 $\pm$ 0.04		
	0 (Gln <sup>79</sup> )	-19 (Asp <sup>317</sup> ) -8 (Leu <sup>328</sup> ) 0 (Tyr <sup>336</sup> ) +9 (Tyr <sup>345</sup> ) +18 (Asn <sup>354</sup> ) +28 (Asp <sup>364</sup> )	<5% 53 $\pm$ 1% 63 $\pm$ 1% 77 $\pm$ 2% 41 $\pm$ 5% 23 $\pm$ 3%	n.d. 4.16 $\pm$ 0.13 2.24 $\pm$ 0.16 0.47 $\pm$ 0.03 0.37 $\pm$ 0.01 0.24 $\pm$ 0.02	cGi-500	
	-6 (Thr <sup>85</sup> )	-8 (Leu <sup>328</sup> ) 0 (Tyr <sup>336</sup> ) +9 (Tyr <sup>345</sup> )	58 $\pm$ 2% 72 $\pm$ 2% 74 $\pm$ 3%	5.64 $\pm$ 0.40 3.06 $\pm$ 0.47 0.75 $\pm$ 0.21	cGi-6000 cGi-3000	
	-17 (Glu <sup>96</sup> )	0 (Tyr <sup>336</sup> ) +9 (Tyr <sup>345</sup> )	22 $\pm$ 3% 25 $\pm$ 3%	0.49 $\pm$ 0.02 0.13 $\pm$ 0.01		
	cNMP-BD A (Gln <sup>79</sup> – Asn <sup>228</sup> )	+5 (Phe <sup>74</sup> )	+5 (Leu <sup>233</sup> )	<5%	n.d.	
		0 (Gln <sup>79</sup> )	+5 (Leu <sup>233</sup> ) +16 (Asn <sup>244</sup> ) +28 (Asp <sup>256</sup> )	<5% <5% <5%	n.d. n.d. n.d.	

**Table 3** Dynamic range and affinity of cGMP sensors

Dynamic ranges and affinities ( $EC_{50}$ ) of all cGMP sensors described so far and reported in this manuscript are shown. To facilitate comparison, either the YFP/CFP (Y/C) or the CFP/YFP (C/Y) emission ratio changes are listed, whichever is larger for a given sensor, i.e. YFP/CFP is given for constructs that show cGMP-induced FRET increases and CFP/YFP for constructs showing cGMP-induced FRET decreases. n.d., value missing in the reference cited.

parent protein	sensor	cGMP effect		reference
		FRET change	$EC_{50}$ ( $\mu$ M)	
cGK	cgy-Del1	24% <sup>Y/C</sup>	n.d.	[29]
	cygnet	40% <sup>C/Y</sup>	1.9 $\mu$ M	[30]
	cGES-GKIB	n.d.	5 $\mu$ M	[31]
	cGi-500	77% <sup>C/Y</sup>	0.5 $\mu$ M	
	cGi-3000	72% <sup>C/Y</sup>	3 $\mu$ M	
	cGi-6000	58% <sup>C/Y</sup>	6 $\mu$ M	
PDE5	cGES-DE5	16% <sup>Y/C</sup>	1.5 $\mu$ M	supplement to [31]

## FIGURE LEGENDS

### Figure 1 Schematic domain structure of cGMP indicators

All indicators are composed of a fragment of a cGMP-binding protein sandwiched between the cyan fluorescent protein (CFP) and the yellow fluorescent protein (YFP). Shown are cGMP sensors already published (upper panel) and the ones described in this manuscript (lower panel). The cGMP-binding proteins the indicators were derived from are given on the left; the sensors' names on the right. The sensors contain the cGMP-binding sites cNMP-BD (cGKI) or GAF (PDE5) either as a single site A or B or as tandem of A + B. The numbers indicate the N- and C-terminal amino acids of the cGMP-binding domain used. The first cGMP sensors, 'cygnet' and 'egy' were derived from cGKI with only 78 or 47 N-terminal amino acids deleted. cGES-GKIB and cGES-DE5 are composed of a single cGMP-binding site of either cGKI or PDE5, respectively. The general design of constructs characterized in this manuscript is given in the lower panel. The boxes represent the regions of the parent proteins adjoining the cGMP-binding domains. From PDE5, either the tandem of GAF A + B or the isolated GAF A were used and shortened or elongated by the amino acids indicated by the arrows. The same strategy was applied to the cNMP-BD of cGKI, again a range of different constructs was created as indicated by the arrows. The PDE5 phosphorylation site is indicated by (P).

### Figure 2 Ligand binding characteristics of a cGMP-sensitive construct designed from the tandem of PDE5 GAF A + B

(A) Concentration response curves of PDE5-GAF A + B (N-terminally elongated by 51 amino acids and C-terminally shortened by 2 amino acids) for cGMP and cAMP were determined *in vitro* from the change in emission ratio at 475 nm (CFP emission) to 525 nm (YFP emission). (b) Binding kinetics at 0.1 to 10  $\mu$ M cGMP were recorded at 525 nm (YFP) by using a rapid mixing device. Please note the different time scales. Original trace data (gray lines) were fitted with single exponential kinetics (black lines) and yielded half lives of approx. 0.7, 14, and 120 s at 10, 1 and 0.1  $\mu$ M cGMP, respectively. (c) Dissociation of cGMP was assessed as emission ratio change after a 100-fold dilution following binding of 1  $\mu$ M cGMP. Original trace data (gray) were fitted with single exponential kinetics (black); the half life was approx 10 min.

### Figure 3 Properties of the cGMP indicators cGi-500, -3000 and -6000

cGMP (A) and cAMP (B) affinities of the indicators cGi-500 (●), -3000 (◆) and -6000 (▲) were determined *in vitro* from the change in CFP to YFP emission ratio. For easier comparison, the ratio changes were normalized to the initial value determined in the absence of cGMP. (C) Dissociation of cGMP from cGi-500 was recorded after a 100-fold dilution to

lower the cGMP concentration. Dissociation was complete within the mixing time when cGMP was lowered from 2.5  $\rightarrow$  0.025  $\mu$ M. As controls, the cGMP concentration was lowered from 250  $\rightarrow$  2.5  $\mu$ M leaving the indicator nearly saturated (compare to panel **a**), and a 100-fold dilution was performed in the absence of cGMP (0  $\rightarrow$  0).

#### **Figure 4**      **cGMP signals in living cells**

cGMP signals in HEK cells stably expressing the NO receptor GC and PDE5 were elicited by NO and YC-1 (indicated by arrows) and recorded by RIA (**A**) and fluorescence microscopy using the cGMP indicators cGi-500 (**B**), -3000 (**C**) and -6000 (**D**). Panels **B-D** show the simultaneously registered mean CFP and YFP emissions (cyan and yellow, respectively) and the mean CFP/YFP emission ratio (black) of the viewing field depicted in the right panel, each normalized to the baseline before application of NO (see *Materials and Methods*). The second ordinate gives the intracellular cGMP concentrations calibrated as described in the *Materials and Methods* section. Representative ratiometric images underlying the black CFP/YFP emission ratio curves at the time points indicated by red arrowheads are shown on the right.

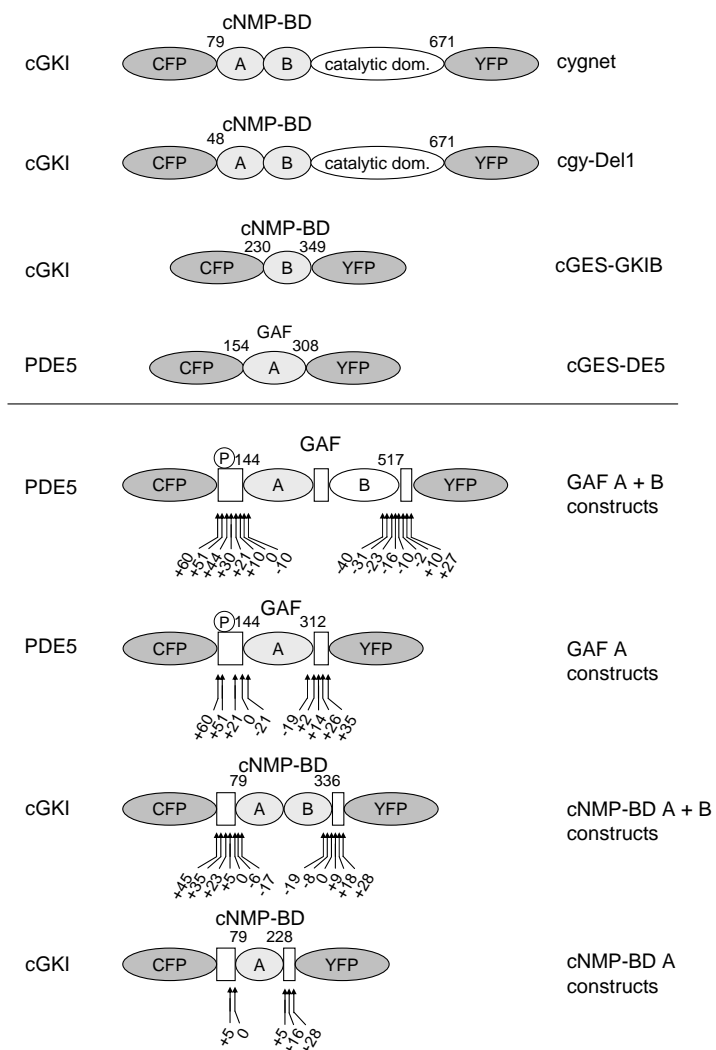


Fig. 1, Russwurm et al.

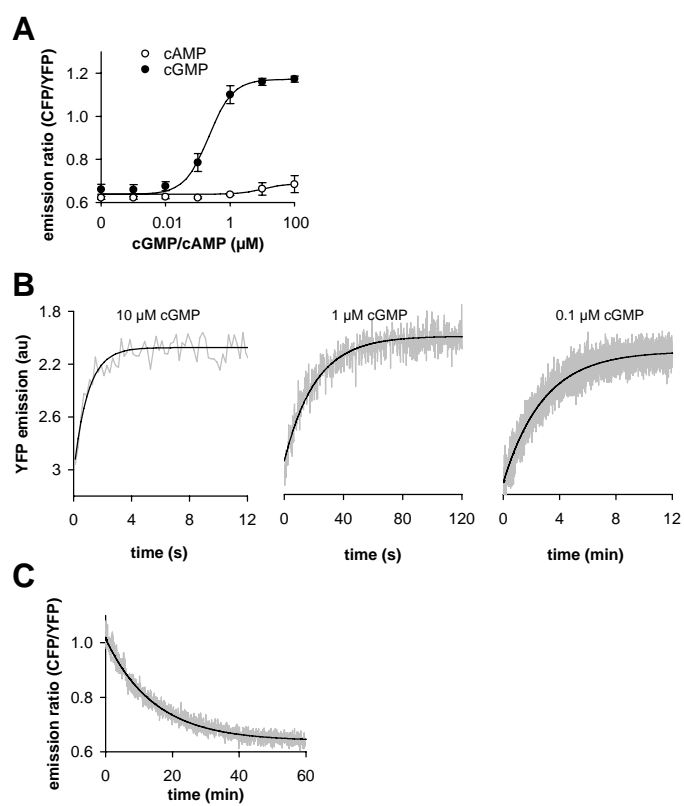


Fig. 2, Russwurm et al.

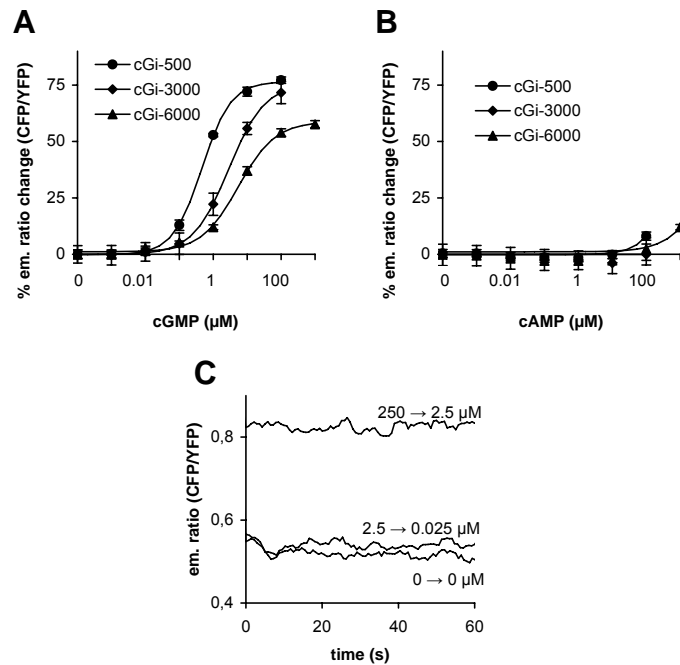


Fig. 3, Russwurm et al.

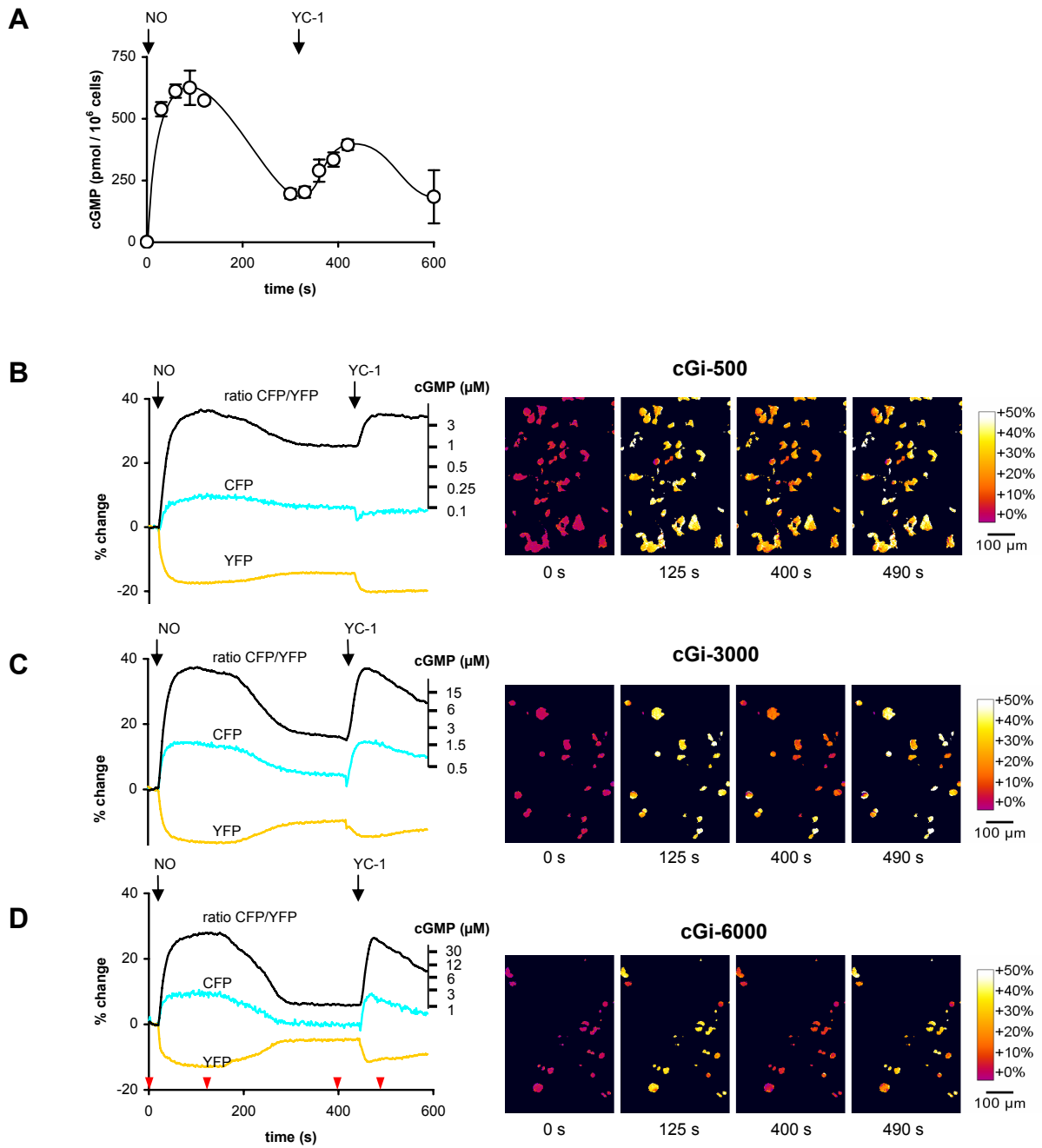


Fig. 4, Russwurm et al.